

## New thermodynamic data for diaspore and their application to the system $\text{Al}_2\text{O}_3\text{-SiO}_2\text{-H}_2\text{O}^1$

DEXTER PERKINS III, ERIC J. ESSENE

*Department of Geology and Mineralogy, The University of Michigan  
Ann Arbor, Michigan 48109*

EDGAR F. WESTRUM, JR.

*Department of Chemistry, The University of Michigan  
Ann Arbor, Michigan 48109*

AND VICTOR J. WALL

*Monash University, Department of Geology  
Clayton, Victoria, Australia*

### Abstract

Recent low-temperature, heat-capacity measurements have been combined with medium-temperature differential scanning calorimetric measurements to yield reliable thermodynamic values for diaspore up to 525 K (251.85°C);  $S_{298,15} = 8.446 \text{ cal K}^{-1} \text{ mole}^{-1}$  and  $H_{298,15} - H_0 = 1683.3 \text{ kcal mole}^{-1}$ . In conjunction with other recent heat-capacity measurements, these data fill many of the remaining gaps in our knowledge of the thermodynamic properties of minerals in the  $\text{Al}_2\text{O}_3\text{-SiO}_2\text{-H}_2\text{O}$  system. By combining thermodynamic data with experimentally determined phase equilibria, several phase diagrams for the  $\text{Al}_2\text{O}_3\text{-SiO}_2\text{-H}_2\text{O}$  system have been modeled. Published reports of naturally occurring assemblages have permitted critical evaluation of each model; a model based upon experiments by Thompson (1970) and Haas and Holdaway (1973) best explains occurrences of pyrophyllite-diaspore and kaolinite-quartz- $\text{Al}_2\text{SiO}_5$ .

### Introduction

Minerals whose compositions lie within the system  $\text{Al}_2\text{O}_3\text{-SiO}_2\text{-H}_2\text{O}$  are present in a wide variety of metamorphic rocks. The occurrences of  $\text{Al}_2\text{SiO}_5$  polymorphs are legion; Zen (1961) has reported many assemblages containing pyrophyllite and kaolinite from greenschist facies rocks in North Carolina; reports of metamorphosed bauxite deposits in Japan are common in the literature. A complete understanding of phase relations in this system has, however, been difficult to achieve due to disagreement among available experimental results and incomplete thermodynamic data for the phases in-

involved. The entropy data for diaspore presented in this paper, in conjunction with recent studies on pyrophyllite by Robie (personal communication) have filled some of the remaining gaps in our knowledge of the thermodynamic properties of minerals within this system.

### Methods

#### *Sample provenance and characterization*

The 58.67 g sample of diaspore from Chester, Massachusetts, used for our heat capacity measurements was light gray in color and almost transparent. The material was obtained from the Mineral Collection of The University of Michigan. Optical, microprobe, and X-ray determinations revealed the presence of minor amounts of chlorite, rutile, and hematite. The

<sup>1</sup> Contribution No. 345 from the Mineralogical Laboratory, Department of Geology and Mineralogy, The University of Michigan, Ann Arbor, Michigan 48109.

chlorite was easily removed since it coated the diaspo-re vein. The rutile appeared to occur as primary inclusions in the diaspo-re and was scattered throughout the material; the hematite tended to be concentrated along fractures and cleavage traces. The sample was broken to flakes of 5 to 10 mm square and 1 to 3 mm thick. The transparent nature of the material allowed easy removal of pieces containing the foreign phases.

Major and minor element analyses were obtained using an ARL-EMX microprobe. Oxide standards were used for Al, Mg, Mn, Fe, and Si. An aluminous pyroxene was used as standard for Ca, a fluoroapatite for F, and a kaersutite for Ti.<sup>2</sup> Accelerating voltage, digitized emission current, and sample current were typically 10 keV, 150  $\mu$ A, and 0.006  $\mu$ A respectively. Counting times were 30–40 seconds for each spot; 10 spots on each of 4 flakes were analyzed. Counts were measured using wavelength-dispersive PET, LIF, and TAP crystals, and all data were reduced by the computer program EMPADR VII of Rucklidge and Gasparrini (1969).<sup>3</sup> The analytical results, normalized on O = OH + F = 1 (Table 1) varied by less than 1 percent for all individual spots.

#### Calorimetric technique

Heat capacity measurements were made in the Mark-II adiabatic cryostat over the range 5 to 350 K. Details of cryostat construction and measuring-circuit calibration have been described elsewhere (Westrum *et al.*, 1968). Samples were measured in the gold-plated copper calorimeter (laboratory designation W-52) which has an internal volume of 59.1 cm<sup>3</sup> and an axial entrant well for the thermometer-heat assembly. After evacuation of the calorimeter containing the sample, 15 kPa of helium gas was added to enhance thermal contact and reduce equilibration times between calorimeter, sample, and the heater/thermometer assembly. Temperatures were measured with a capsule-type platinum resistance thermometer (A-3) calibrated by the National Bureau of Standards. The calibration is referred to as the International Practical Temperature Scale, IPTS-48, text revision of Stimson (1961), defined between

<sup>2</sup> The pyroxene and kaersutite standards and analyses were obtained from A. J. Irving, Lunar Science Institute, Houston. The apatite standard and analysis was obtained from B. W. Evans, University of Washington, Seattle.

<sup>3</sup> Includes corrections for atomic number, mass absorption, and fluorescence.

Table 1. Microprobe analysis of Chester diaspo-re

| Oxide                          | wt. %  | Ion              | No. ions | End member       | %    |
|--------------------------------|--------|------------------|----------|------------------|------|
| Al <sub>2</sub> O <sub>3</sub> | 85.02  | Al               | 0.995    | AlO(OH)          | 99.5 |
| Fe <sub>2</sub> O <sub>3</sub> | 0.58   | Fe <sup>3+</sup> | 0.005    | FeO(OH)          | 0.5  |
| Mn <sub>2</sub> O <sub>3</sub> | 0.03   | Mn <sup>3+</sup> | <0.001   | MnO(OH)          | <0.1 |
| MgO                            | —      | Mg               | —        | MgO(OH)          | —    |
| CaO                            | 0.07   | Ca               | <0.001   | CaO(OH)          | <0.1 |
| TiO <sub>2</sub>               | 0.06   | Ti               | <0.001   | TiO <sub>2</sub> | <0.1 |
| SiO <sub>2</sub>               | —      | Si               | —        | SiO <sub>2</sub> | —    |
| F                              | 0.02   | F                | <0.001   | AlO(F)           | <0.1 |
| H <sub>2</sub> O <sup>a</sup>  | 15.11  | OH               | 1.000    | —                | —    |
|                                | 100.84 | O =              | 1.000    |                  |      |

a) H<sub>2</sub>O determined by stoichiometry

90.18 and 903.65 K. The National Bureau of Standards 1955 provisional scale was employed at lower temperatures.

A molar mass of 59.9883 g, corresponding to the formula AlO(OH), was used for the calculation of apparent heat capacity (Table 3) from the observed values of the heat capacity of the sample. Measured heat capacities were corrected for the heat capacity of the empty calorimeter, which was determined in a separate series of experiments. Slight adjustments were made for the differences in the amount of gaseous helium used with the calorimeter when it was run empty and when loaded with diaspo-re.

Heat capacities from 325 to 520 K were measured in a Perkin-Elmer differential scanning calorimeter (Model DSC-2) in R. A. Robie's laboratory at the U. S. Geological Survey in Reston, Virginia. A 33.13 mg sample of diaspo-re and a 30.66 mg sample of corundum (NBS Heat Capacity Standard Reference Material No. 270) were loaded into gold containers of approximately 130 mg each. Three overlapping scans of 115, 110, and 120 K were made to a maximum temperature of 520 K at a heating rate of 10 K/minute. Attempts to make an additional determination above 520 K resulted in partial dehydration of the diaspo-re sample. Temperatures were calibrated against the known transition temperatures of In and KClO<sub>4</sub>. All data were processed by the computer program DSC-7B (Krupka, 1975, written communication) which utilized, as a standard, the heat capacity of corundum from Ditmars and Douglas (1971).

Table 2. Experimental low-temperature heat capacity of dias-pore\*

| $\frac{T}{K}$ | $\frac{C_p}{\text{cal K}^{-1} \text{mole}^{-1}}$ | $\frac{T}{K}$ | $\frac{C_p}{\text{cal K}^{-1} \text{mole}^{-1}}$ | $\frac{T}{K}$ | $\frac{C_p}{\text{cal K}^{-1} \text{mole}^{-1}}$ |
|---------------|--------------------------------------------------|---------------|--------------------------------------------------|---------------|--------------------------------------------------|
| Series I      |                                                  |               |                                                  |               |                                                  |
|               | 203.74                                           | 8.473         |                                                  | 8.18          | 0.00147                                          |
|               | 213.83                                           | 9.007         |                                                  | 9.27          | 0.00185                                          |
| 62.04         | 0.6057                                           | 223.93        | 9.516                                            | 10.33         | 0.00248                                          |
| 70.48         | 0.885                                            | 234.04        | 10.012                                           | 11.60         | 0.00342                                          |
| 72.29         | 1.1569                                           | 244.17        | 10.514                                           | 12.92         | 0.00479                                          |
| 86.61         | 1.586                                            | 254.39        | 11.000                                           | 14.37         | 0.00647                                          |
| 96.61         | 2.097                                            | 264.60        | 11.467                                           | 15.94         | 0.00912                                          |
| 106.63        | 2.655                                            | 274.67        | 11.874                                           | 17.59         | 0.01171                                          |
| 116.25        | 3.301                                            | 284.69        | 12.235                                           | 19.31         | 0.01547                                          |
| 125.42        | 3.794                                            | 294.70        | 12.611                                           | 21.14         | 0.02048                                          |
| 135.51        | 4.422                                            | 304.75        | 12.980                                           | 23.14         | 0.02701                                          |
| Series II     |                                                  |               |                                                  |               |                                                  |
|               | 314.94                                           | 13.335        |                                                  | 25.36         | 0.03539                                          |
|               | 325.21                                           | 13.671        |                                                  | 27.90         | 0.04809                                          |
|               | 335.37                                           | 14.021        |                                                  | 30.68         | 0.06561                                          |
| 135.98        | 4.452                                            | 345.35        | 14.343                                           | 33.71         | 0.08731                                          |
| 124.01        | 5.081                                            |               |                                                  | 36.60         | 0.11518                                          |
| 155.87        | 5.694                                            | Series III    |                                                  | 39.51         | 0.1449                                           |
| 165.33        | 6.288                                            |               |                                                  | 43.29         | 0.1919                                           |
| 174.65        | 6.837                                            | 4.79          | 0.00045                                          | 47.55         | 0.2617                                           |
| 183.90        | 7.359                                            | 6.23          | 0.00050                                          | 51.43         | 0.3351                                           |
| 193.68        | 7.912                                            | 7.28          | 0.00095                                          | 56.03         | 0.4414                                           |
|               |                                                  |               |                                                  | 61.80         | 0.6007                                           |

\*  $A_{10}(\text{OH})$ ; mol = 59.988 g;  
cal = 4.184 J.

## Results

### Heat capacity

Values for the individual determinations of heat capacity are presented in Tables 2 and 3 in chronological sequence at the mean temperatures of each determination. Hence, the temperature increments utilized for the individual determinations within a series may be deduced from the differences between the adjacent mean temperatures. An analytically determined curvature correction has been applied to the measured values of  $\Delta H/\Delta T$  in non-transitional regions (*cf.* Westrum *et al.*, 1968). These results were considered to be characterized by a standard deviation of about 5 percent near 10 K, decreasing to about 0.8 percent at 20 K and to less than 0.1 percent from 30 K to 350 K. The precision of all DSC mea-

surements above 350 K (estimated on the basis of overlapping scans) was better than 0.8 percent; the accuracy is considered to be about 1 percent (Robie, personal communication).

### Thermodynamic properties

The heat capacity values below 10 K were extrapolated by the expression  $C_p = AT^3$  (*cf.* Westrum *et al.*, 1968). Values of the several thermodynamic properties are given in Table 4 at selected temperatures. These functions were obtained by computer integration of the smoothed heat capacity curve, values of which are cited in the first column. The thermodynamic functions obtained by integration are listed in the other columns of the table.

Because the composition of the sample deviated slightly from that of ideal dias-pore, an adjustment to correct the smooth thermodynamic functions to those characteristic of pure dias-pore was made. The approximation, involving the compositions of the end members of solutions composing the natural dias-pore, has been described by Westrum *et al.* (1978). The relevant end members and their mole fractions are cited in Table 1.

Since the sample has only one impurity of any significance,  $\text{FeO}(\text{OH})$ , the entropy adjustment at 298.15 K is simply:

$$S_{\text{corr}}^{\circ} = (S_{\text{obs}}/W) - 0.005 \cdot 1/2 \cdot (S_{\text{Fe}_2\text{O}_3} - S_{\text{Al}_2\text{O}_3})$$

in which 0.005 is the mole fraction of  $\text{FeO}(\text{OH})$ , and  $W$  (the ratio of the molecular weight of pure dias-pore to that of the sample) = 0.9962 and thus since  $S_{\text{obs}}^{\circ} = 8.44_6 \text{ cal K}^{-1} \text{ mole}^{-1}$ ,  $S_{\text{corr}}^{\circ} = 8.44_4 \text{ cal K}^{-1} \text{ mole}^{-1}$  (using the data of Robie and Waldbaum, 1968). Similar checks for the other thermodynamic functions (and  $C_p$ ) were made; the correction terms were always well within the experimental precision, and further adjustments were not made.

Earlier measurements by King *et al.* (1967) on the entropy of dias-pore yielded a value of  $8.42 \pm 0.03 \text{ cal K}^{-1} \text{ mole}^{-1}$  at 298.15 K. Although the entropy at 298.15 K from our measurements differs from that of King *et al.* by only about 0.4 percent, our heat capacity is about 6 percent lower than theirs near 51 K (their lowest temperature of measurement). This deviation decreases, becomes zero, and then increases steadily to 1.1 percent higher at 300 K, possibly as a consequence of the large corrections they made for impurities and their lack of data below 51 K. Comparison of our medium-temperature (350 K–520 K) values with those of Mukaibo and Takahashi (1969)

Table 3. DSC determined heat capacities of dias-pore\*

| $\frac{T}{K}$ | $\frac{C_p}{\text{cal K}^{-1} \text{mole}^{-1}}$ | $\frac{T}{K}$ | $\frac{C_p}{\text{cal K}^{-1} \text{mole}^{-1}}$ | $\frac{T}{K}$ | $\frac{C_p}{\text{cal K}^{-1} \text{mole}^{-1}}$ |
|---------------|--------------------------------------------------|---------------|--------------------------------------------------|---------------|--------------------------------------------------|
| 340.08        | 14.02                                            | 409.88        | 15.81                                            | 459.42        | 17.64                                            |
| 350.01        | 14.30                                            | 419.70        | 16.04                                            | 459.52        | 16.74                                            |
| 369.86        | 14.91                                            | 419.81        | 16.09                                            | 469.34        | 17.10                                            |
| 389.72        | 15.30                                            | 429.42        | 16.28                                            | 479.30        | 17.23                                            |
| 389.92        | 15.33                                            | 439.56        | 16.47                                            | 499.24        | 17.57                                            |
| 399.85        | 15.59                                            | 439.66        | 16.44                                            | 509.16        | 17.77                                            |
| 409.58        | 15.75                                            |               |                                                  |               |                                                  |

shows their values deviate by up to 3 percent from ours at certain temperatures. The scatter in their data is most likely a result of the smaller sample (5.276 g) they used, coupled with the experimental uncertainties of their continuous heating adiabatic calorimetric technique and the possibility that equilibrium was not attained.

The entropy of diaspoire is significantly less than that of boehmite, another  $\text{AlO}(\text{OH})$  polymorph, presumably due to diaspoire's greater density. Both structures involve octahedrally-coordinated aluminum atoms between layers of oxygen atoms. However, in diaspoire the oxygen atoms are hexagonally closest packed, while in boehmite they are cubic closest packed. A similar relationship holds between their dehydration products—diaspoire dehydrates to  $\alpha\text{-Al}_2\text{O}_3$  (corundum), while boehmite dehydrates to  $\gamma\text{-Al}_2\text{O}_3$ .

### Discussion

#### *The stabilities of diaspoire, boehmite, gibbsite and bayerite*

Although both diaspoire and boehmite are common in bauxites and laterites, thermodynamic considerations imply that boehmite is always metastable. Heat of dehydration measurements (Mukaibo and Takahashi, 1969) indicate that diaspoire is the more stable polymorph by 3.65 kcal at 500 °C. If the approximation  $\Delta S_r^\circ = \Delta S_{298,15}^\circ$  (Table 5) is used, the location of the equilibrium boundary diaspoire = boehmite can be calculated (using the data of Robie and Waldbaum, 1968) to be approximately 1600°C at 1 atmosphere. Moreover, both  $\Delta S_r$  and  $\Delta V_r$  are positive for this reaction. Thus it has a positive slope in pressure-temperature space, and is always (Fig. 1) on the high-temperature side of the reaction:



as determined by Fyfe and Hollander (1964) and by Haas (1972). It is unlikely, therefore, that a stability field exists for boehmite within geologic pressure/temperature ranges. This conclusion is in agreement with those of Kennedy (1959), of Neuhaus and Heide (1969), and of Day (1975, 1976).

Limits on the stabilities of gibbsite and bayerite have been determined by Ervin and Osborn (1951) and Kennedy (1959). In studies on the reaction:



Ervin and Osborn were able to grow boehmite from

Table 4. Thermodynamic properties of diaspoire at selected temperatures

| $\frac{T}{K}$ | $\frac{C_p}{\text{cal K}^{-1} \text{mole}^{-1}}$ | $\frac{S^\circ}{\text{cal K}^{-1} \text{mole}^{-1}}$ | $\frac{H^\circ - H^\circ_0}{\text{cal mole}^{-1}}$ | $\frac{-(G^\circ - H^\circ_0)/T}{\text{cal K}^{-1} \text{mole}^{-1}}$ |
|---------------|--------------------------------------------------|------------------------------------------------------|----------------------------------------------------|-----------------------------------------------------------------------|
| 5             | 0.0003                                           | 0.0001                                               | 0.0004                                             | 0.0000                                                                |
| 10            | 0.0022                                           | 0.0007                                               | 0.0054                                             | 0.0000                                                                |
| 15            | 0.0078                                           | 0.0026                                               | 0.0292                                             | 0.0006                                                                |
| 20            | 0.0171                                           | 0.0060                                               | 0.0890                                             | 0.0015                                                                |
| 25            | 0.0346                                           | 0.0115                                               | 0.2153                                             | 0.0029                                                                |
| 30            | 0.0606                                           | 0.0200                                               | 0.4492                                             | 0.0050                                                                |
| 35            | 0.0981                                           | 0.0320                                               | 0.8405                                             | 0.0080                                                                |
| 40            | 0.1503                                           | 0.0483                                               | 1.4549                                             | 0.0119                                                                |
| 45            | 0.2194                                           | 0.0698                                               | 2.372                                              | 0.0171                                                                |
| 50            | 0.3076                                           | 0.0973                                               | 3.681                                              | 0.0237                                                                |
| 60            | 0.5462                                           | 0.1732                                               | 7.879                                              | 0.0419                                                                |
| 70            | 0.8702                                           | 0.1806                                               | 14.891                                             | 0.0679                                                                |
| 80            | 1.2752                                           | 0.4224                                               | 25.554                                             | 0.1030                                                                |
| 90            | 1.750                                            | 0.5994                                               | 40.629                                             | 0.1480                                                                |
| 100           | 2.282                                            | 0.8109                                               | 60.79                                              | 0.2034                                                                |
| 110           | 2.855                                            | 1.0550                                               | 86.41                                              | 0.2695                                                                |
| 120           | 3.457                                            | 1.3291                                               | 117.95                                             | 0.3462                                                                |
| 130           | 4.074                                            | 1.630                                                | 155.61                                             | 0.4332                                                                |
| 140           | 4.704                                            | 1.955                                                | 199.48                                             | 0.5302                                                                |
| 150           | 5.337                                            | 2.301                                                | 249.69                                             | 0.6366                                                                |
| 160           | 5.958                                            | 2.666                                                | 306.18                                             | 0.7520                                                                |
| 170           | 6.560                                            | 3.045                                                | 368.78                                             | 0.8756                                                                |
| 180           | 7.143                                            | 3.436                                                | 437.31                                             | 1.0070                                                                |
| 190           | 7.709                                            | 3.838                                                | 511.6                                              | 1.1454                                                                |
| 200           | 8.259                                            | 4.247                                                | 591.4                                              | 1.2902                                                                |
| 210           | 8.796                                            | 4.663                                                | 676.7                                              | 1.4409                                                                |
| 220           | 9.320                                            | 5.085                                                | 767.3                                              | 1.597                                                                 |
| 230           | 9.830                                            | 5.510                                                | 863.1                                              | 1.758                                                                 |
| 240           | 10.322                                           | 5.939                                                | 963.9                                              | 1.923                                                                 |
| 250           | 10.795                                           | 6.370                                                | 1069.5                                             | 2.092                                                                 |
| 260           | 11.245                                           | 6.802                                                | 1179.7                                             | 2.265                                                                 |
| 270           | 11.670                                           | 7.235                                                | 1294.3                                             | 2.441                                                                 |
| 273.15        | 11.799                                           | 7.371                                                | 1331.2                                             | 2.497                                                                 |
| 280           | 12.072                                           | 7.667                                                | 1413.0                                             | 2.620                                                                 |
| 290           | 12.451                                           | 8.097                                                | 1535.6                                             | 2.802                                                                 |
| 298.15        | 12.746                                           | 8.446                                                | 1638.3                                             | 2.951                                                                 |
| 300           | 12.811                                           | 8.525                                                | 1661.9                                             | 2.985                                                                 |
| 310           | 13.159                                           | 8.951                                                | 1791.8                                             | 3.171                                                                 |
| 320           | 13.500                                           | 9.473                                                | 1925.1                                             | 3.358                                                                 |
| 330           | 13.820                                           | 9.795                                                | 2061.8                                             | 3.547                                                                 |
| 340           | 14.140                                           | 10.213                                               | 2201.8                                             | 3.737                                                                 |
| 350           | 14.421                                           | 10.628                                               | 2345.2                                             | 3.928                                                                 |
| 360           | 14.65                                            | 11.04                                                | 2490.0                                             | 4.12                                                                  |
| 370           | 14.90                                            | 11.44                                                | 2638.0                                             | 4.31                                                                  |
| 380           | 15.14                                            | 11.84                                                | 2788.0                                             | 4.50                                                                  |
| 390           | 15.37                                            | 12.24                                                | 2940.0                                             | 4.70                                                                  |
| 400           | 15.59                                            | 12.63                                                | 3095.0                                             | 4.90                                                                  |
| 410           | 15.81                                            | 13.02                                                | 3252.0                                             | 5.09                                                                  |
| 420           | 16.03                                            | 13.40                                                | 3412.0                                             | 5.28                                                                  |
| 430           | 16.24                                            | 13.78                                                | 3573.0                                             | 5.47                                                                  |
| 440           | 16.45                                            | 14.15                                                | 3736.0                                             | 5.66                                                                  |
| 450           | 16.66                                            | 14.53                                                | 3902.0                                             | 5.86                                                                  |
| 460           | 16.86                                            | 14.90                                                | 4070.0                                             | 6.05                                                                  |
| 470           | 17.05                                            | 15.26                                                | 4239.0                                             | 6.24                                                                  |
| 480           | 17.24                                            | 15.62                                                | 4411.0                                             | 6.43                                                                  |
| 490           | 17.42                                            | 15.98                                                | 4584.0                                             | 6.62                                                                  |
| 500           | 17.60                                            | 16.33                                                | 4759.0                                             | 6.82                                                                  |
| 510           | 17.77                                            | 16.68                                                | 4936.0                                             | 7.01                                                                  |
| 520           | 17.96                                            | 17.03                                                | 5115.0                                             | 7.19                                                                  |

gibbsite at 140°C and pressures below 1 kbar. Thermodynamic calculations (assuming  $\Delta S_r$  and  $\Delta V_r$  for the solids are constant) show this reaction to have a steep positive slope at 140°C (Fig. 1), although its ex-

Table 5. Entropies and volumes of diaspore, boehmite, gibbsite, and bayerite at 298.15K

| Mineral  | Composition                    | $S$                                  |  | $V$                   |  |
|----------|--------------------------------|--------------------------------------|--|-----------------------|--|
|          |                                | $\text{cal K}^{-1} \text{mole}^{-1}$ |  | $\text{cc mole}^{-1}$ |  |
| Diaspore | $\alpha\text{-AlO}(\text{OH})$ | 8.44 <sup>a</sup>                    |  | 17.76 <sup>b</sup>    |  |
| Boehmite | $\gamma\text{-AlO}(\text{OH})$ | 11.58 <sup>b</sup>                   |  | 19.53 <sup>b</sup>    |  |
| Gibbsite | $\text{Al}(\text{OH})_3$       | 16.75 <sup>b</sup>                   |  | 32.00 <sup>b</sup>    |  |
| Bayerite | $\text{Al}(\text{OH})_3$       | 16.05 <sup>c</sup>                   |  | 31.15 <sup>d</sup>    |  |

- a) This study  
 b) Robie and Waldbaum (1968)  
 c) Shomate and Cook (1946)  
 d) Rothbauer et al. (1967)

act location cannot be accurately determined due to uncertainties in the thermal expansivities and compressibilities of the phase involved. However, a stability field for gibbsite, if it exists, must be on the low-temperature side of this reaction. Day (1976) has made calculations of  $\Delta G_r$  which indicate that the reaction would take place at extremely low temperature if at all, although the uncertainties in his calculations were greater than the  $\Delta G_r$  that he calculated. For metamorphic pressures ( $P > 1$  kbar) and temperatures ( $T > 100^\circ\text{C}$ ), then, it seems reasonable to consider diaspore as the only stable aluminum-hydrate mineral. Indeed, geologic occurrences of the other alumina-hydrates are in low-temperature environments where metastability is to be expected.

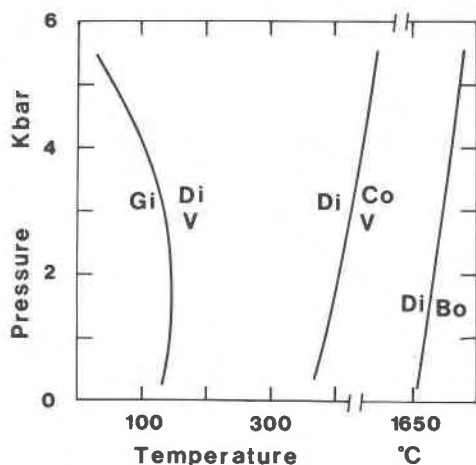


Fig. 1. Schematic diagram of phase relations in the  $\text{Al}_2\text{O}_3\text{-H}_2\text{O}$  system. Abbreviations: Di = diaspore, Co = corundum, Gi = gibbsite, Bo = boehmite, V =  $\text{H}_2\text{O}$ .

### Phase equilibria in the system $\text{Al}_2\text{O}_3\text{-SiO}_2\text{-H}_2\text{O}$

We have considered 26 reactions (Table 6) and 9 phases (Fig. 2) within the  $\text{Al}_2\text{O}_3\text{-SiO}_2\text{-H}_2\text{O}$  system. Thermodynamic calculations were made using the computer program EQUILI of Wall and Essene (unpublished). Given an initial  $\Delta G_r(P_1, T_1)$ ,  $\Delta G_r(P_2, T_2)$  was calculated as follows:

$$\Delta G_r(P_2, T_2) = \Delta G_r(P_1, T_1) + \left[ \int_{P_1}^{P_2} \Delta V_r dP - \int_{T_1}^{T_2} \Delta S_r dT \right]_{\text{solids}} + n[G(P_2, T_2) - G(P_1, T_1)]_{\text{H}_2\text{O}}$$

in which:

$\Delta G_r(P, T)$  = Gibbs energy of reaction at pressure  $P$ , and temperature  $T$

$\Delta V_r$  = volume change of reaction

$\Delta S_r$  = entropy change of reaction

$n$  = number of moles of water in products minus that in the reactants

In order to evaluate  $\Delta V_r(P, T)$  and  $\Delta S_r(P, T)$ , thermal expansion ( $\alpha$ ) and compressibility ( $\beta$ ) were used to calculate  $V(P, T)$  and  $S(P, T)$  for solid phases as follows:

$$V(P, T) = V^\circ(298.15) + \int_{298.15}^T \alpha V dT - \int_{1 \text{ atm}}^P \beta V dP$$

$$S(P, T) = S^\circ(T) - \int_{1 \text{ atm}}^P \alpha V dP$$

It was assumed that  $\alpha(P, T) = \alpha^\circ(T)$  and  $\beta(P, T) = \beta^\circ(298.15)$ . All  $V^\circ$  values were taken from Robie et al. (1967).  $\alpha$  and  $\beta$  were taken from Skinner and Birch (in Clark, 1966) or estimated on the basis of data on minerals of similar crystal structure.<sup>4</sup>  $S^\circ(T)$  values were taken directly from Robie and Waldbaum (1968) for all solids except diaspore, kaolinite and pyrophyllite. The diaspore values were our own; the pyrophyllite values were from Robie (personal communication). The kaolinite entropies (Table 7) were determined by combining the  $S_{298.15}^\circ$  value in Robie and Waldbaum (1968) with the approximation:

$$S_T - S_{298.15}|_{\text{Ka}} = S_T - S_{298.15}|_{\text{Sp}} + S_T - S_{298.15}|_{\text{Py}} - S_T - S_{298.15}|_{\text{Te}}$$

<sup>4</sup> Compressibilities of  $\text{Al}_2\text{SiO}_5$  minerals were taken from Brace et al. (1969). Thermal expansivities of diaspore and kaolinite were assumed to be equal to that of pyrophyllite. Compressibilities of diaspore, pyrophyllite, and kaolinite were assumed to be equal to that of muscovite.

Table 6. Standard Gibbs energies of reaction at 25°C (298.15K) and 1 atm

| No. | Reaction                | Source of data           | Model 1 <sup>a</sup> | Model 2 <sup>b</sup> | Model 3 <sup>c</sup> | Model 4 <sup>d</sup> |
|-----|-------------------------|--------------------------|----------------------|----------------------|----------------------|----------------------|
| 1   | Ky = And                | Holdaway                 | -0.42 ± 0.05         | -0.42 ± 0.05         | -0.42 ± 0.05         | -0.42 ± 0.05         |
| 2   | And = Sill              | Holdaway                 | 0.89 ± 0.05          | 0.89 ± 0.05          | 0.89 ± 0.05          | 0.89 ± 0.05          |
| 3   | Ky = Sill               | Holdaway                 | 0.47 ± 0.05          | 0.47 ± 0.05          | 0.47 ± 0.05          | 0.47 ± 0.05          |
| 4   | Py = And + 3Q + V       | Haas & Holdaway, Kerrick | 5.06 ± 0.05          | 5.06 ± 0.05          | 4.41 ± 0.05          | 4.41 ± 0.05          |
| 5   | Py = Ky + 3Q + V        | (4)-(1)                  | 5.48 ± 0.10          | †5.48 ± 0.10         | 4.53 ± 0.10          | 4.83 ± 0.10          |
| 6   | Ka + 2Q = Py + V        | Reed & Hemley, Thompson  | 2.10 ± 0.09          | 1.76 ± 0.05          | 2.10 ± 0.09          | 1.76 ± 0.05          |
| 7   | Py + 6Di = 4And + 4V    | Haas                     | 17.97 ± 0.41         | 17.97 ± 0.41         | 17.97 ± 0.41         | 17.97 ± 0.41         |
| 8   | Py + 6Di = 4Ky + 4V     | (7)-4(1)                 | 19.35 ± 0.60         | 19.35 ± 0.60         | 19.35 ± 0.60         | 19.35 ± 0.60         |
| 9   | 2Di = Co + V            | Haas                     | 5.43 ± 0.07          | 5.43 ± 0.07          | 5.43 ± 0.07          | 5.43 ± 0.07          |
| 10  | Py = 4Q + 2Di           | 1.33(4)-0.33(7)          | 0.75 ± 0.20          | 0.75 ± 0.20          | 0.11 ± 0.20          | -0.11 ± 0.20         |
| 11  | Ka = 2Q + 2Di + V       | (6)+1.33(4)-0.33(7)      | 2.85 ± 0.30          | 2.51 ± 0.25          | 1.99 ± 0.30          | 1.65 ± 0.25          |
| 12  | 2Ka = 2Di + Py + 2V     | 2(6)+1.33(4)-0.33(7)     | 4.95 ± 0.39          | 4.27 ± 0.30          | 4.09 ± 0.39          | 3.40 ± 0.30          |
| 13  | 3Ka = Py + 2Ky + 5V     | (14)-2(1)                | 17.25 ± 0.48         | 16.23 ± 0.35         | 15.96 ± 0.48         | 14.93 ± 0.35         |
| 14  | 3Ka = Py + 2And + 5V    | 3(6)+2(4)                | 16.41 ± 0.38         | 15.39 ± 0.25         | 15.12 ± 0.38         | 14.09 ± 0.25         |
| 15  | Ka + 2Di = 2Ky + 3V     | 16-2(1)                  | 12.30 ± 0.36         | 11.96 ± 0.31         | 11.87 ± 0.36         | 11.53 ± 0.31         |
| 16  | Ka + 2Di = 2And + 3V    | (6)+0.66(4)+0.33(7)      | 11.46 ± 0.26         | 11.12 ± 0.22         | 11.03 ± 0.26         | 10.69 ± 0.22         |
| 17  | 4Ky + 4Ka = 3Py + 10Di  | (18)+4(1)                | -9.75 ± 1.38         | -11.12 ± 1.20        | -11.48 ± 1.38        | -12.85 ± 1.20        |
| 18  | 4And + 4Ka = 3Py + 10Di | 4(6)+2.66(4)-1.66(7)     | -8.07 ± 1.19         | -9.44 ± 1.01         | -9.80 ± 1.19         | -11.16 ± 1.01        |
| 19  | Ka = And + Q + 2V       | (6)+(4)                  | 7.16 ± 0.14          | 6.18 ± 0.14          | 6.51 ± 0.14          | 6.17 ± 0.10          |
| 20  | Ka = Ky + Q + 2V        | (19)-(1)                 | 7.58 ± 0.18          | 9.23 ± 0.13          | 6.93 ± 0.18          | 6.59 ± 0.13          |
| 21  | 2Py = 5Q + And + Ka     | (4)-(6)                  | 2.95 ± 0.14          | 3.30 ± 0.10          | 2.31 ± 0.14          | 2.65 ± 0.10          |
| 22  | 2Py = 5Q + Ky + Ka      | (21)-(1)                 | 3.37 ± 0.19          | 3.72 ± 0.15          | 2.73 ± 0.15          | 3.07 ± 0.15          |
| 23  | Q + 2Di = Ky + V        | (24)-(1)                 | 4.73 ± 0.20          | 4.73 ± 0.20          | 4.53 ± 0.20          | 4.53 ± 0.20          |
| 24  | Q + 2Di = And + V       | 0.33(7)-0.33(4)          | 4.31 ± 0.15          | 4.31 ± 0.15          | 4.52 ± 0.15          | 4.52 ± 0.15          |
| 25  | 4Di + 3Q = Ky + Ka      | (26)-(1)                 | 1.85 ± 0.50          | 2.32 ± 0.45          | 2.95 ± 0.50          | 3.30 ± 0.45          |
| 26  | 4Di + 3Q = And + Ka     | 0.66(7)-(6)-1.66(4)      | 1.46 ± 0.45          | 1.80 ± 0.80          | 2.53 ± 0.45          | 2.88 ± 0.40          |

a) Based upon experiments by Kerrick (1968) and by Thompson (1970)

b) Based upon experiments by Kerrick (1968) and by Reed and Hemley (1966)

c) Based upon experiments by Haas and Holdaway (1973) and by Thompson (1970)

d) Based upon experiments by Haas and Holdaway (1973) and by Reed and Hemley (1966)

where Sp = serpentine, Py = pyrophyllite, and Tc = talc. The serpentine entropy was taken from King *et al.* (1967). All  $G_{H_2O}$  data were taken from Burnham *et al.* (1969).

Table 6 lists the reactions (metastable and stable) considered in this study. The configuration of reactions 1, 2, and 3 (the  $Al_2SiO_5$  phase diagram) is modified after Wall and Essene (1972) and is consistent with Holdaway's (1971) experiments. A small shift in the location of these reactions would have little effect on the others studied because of the small difference in  $\Delta G_r$  of the different aluminosilicates.

Reaction 4,  $Py = And + 3Q + V$ , has been experimentally studied by Kerrick (1968), Haas and Holdaway (1973), and Hemley (written communication). As noted by Robie (written communication), large discrepancies exist between the results of Haas and Holdaway and those of the other studies. There being no *a priori* reason to choose one set of experiments over the other, we have fitted curves (Fig. 3) to both

sets of data. Although still in preliminary form, Hemley's results tend to support those of Kerrick, locating the reaction at 370–380°C at 1 kbar. The curves were fitted to be consistent with entropy and volume data, to fit through as many reversals as possible, and to minimize the difference (in kcal) between the curve and the limits of all reversals. It should be noted that the experimentally-determined curve of Haas and Holdaway is not consistent with thermodynamically-derived slopes. This may be due to the growth of non-stoichiometric pyrophyllite in their run products, which increased the entropy of pyrophyllite relative to those of the other phases or decreased the amount of water released. Direct examination of run products using an electron microprobe or a scanning transmission electron microscope may clarify this problem.

Uncertainties were determined to be 0.0 kcal for the fit to Kerrick's reversals (since there was no leeway in where the curve could be placed) plus 0.01

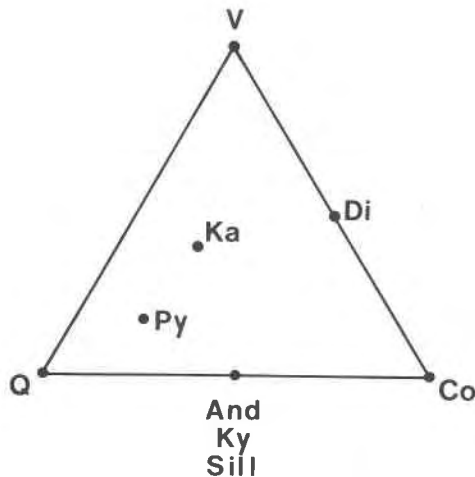


Fig. 2. Stable minerals in the  $\text{Al}_2\text{O}_3\text{-SiO}_2\text{-H}_2\text{O}$  system. Abbreviations as in Fig. 1 and Ka = kaolinite, Py = pyrophyllite, Q = quartz, And = andalusite, Ky = kyanite, Sill = sillimanite. Gibbsite and boehmite have not been included since they are generally not stable (see text).

kcal/mole to account for uncertainties in  $S$  and  $V$ . For models involving data of Haas and Holdaway, the uncertainties listed in Table 6 are the *minimum* shift in the  $\Delta G_r$  necessary to make it consistent with the experiments, plus 0.01 kcal/mole to account for uncertainties in  $S$  and  $V$  for the phases involved.

Reaction 6,  $\text{Ka} + 2\text{Q} = \text{Py} + \text{V}$ , has been studied by Reed and Hemley (1966), Velde and Kornprobst (1969), and Thompson (1970). Reed and Hemley have determined the upper stability of  $\text{Ka} + \text{Q}$  to be  $300^\circ\text{C}$  at 1 kbar. We have arbitrarily placed the reaction at  $295^\circ\text{C}$  and 1 kbar for models involving their study (Fig. 4). Velde and Kornprobst have determined the upper stability for the same assemblage to be at slightly higher temperatures; in neither study was the reaction reversed. Thompson (1970) has reversals at 1, 2, and 4 kbar; we have fitted a curve to his data (Fig. 4) and calculated uncertainties as before. The discrepancy between the locations of the two curves is large and not easily explained.

Reaction 7,  $\text{Py} + 6\text{Di} = 4\text{And} + 4\text{V}$ , has been studied by Haas and Holdaway (1973). A curve fitted

Table 7. Estimated entropy of kaolinite

| $\frac{T}{K}$ | $\frac{S}{\text{cal K}^{-1} \text{mole}^{-1}}$ | $\frac{T}{K}$ | $\frac{S}{\text{cal K}^{-1} \text{mole}^{-1}}$ |
|---------------|------------------------------------------------|---------------|------------------------------------------------|
| 298.15        | 48.53                                          | 600           | 108.23                                         |
| 400           | 71.19                                          | 700           | 123.79                                         |
| 500           | 90.81                                          | 800           | 137.96                                         |

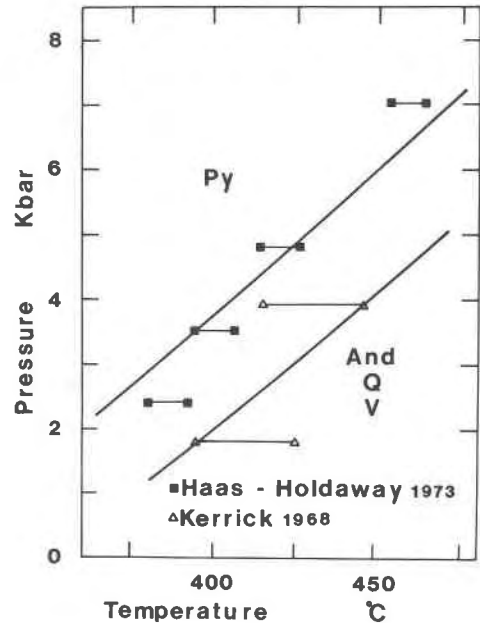


Fig. 3. The reaction  $\text{Py} = \text{And} + 3\text{Q} + \text{V}$ . The solid lines are consistent with available thermodynamic data. For simplicity the reactant and product assemblages are only shown once in this and the next figure.

to their data (Fig. 5) passes through all reversals. Reaction 9, the breakdown of diaspore to corundum plus water, has been studied by Fyfe and Hollander (1964), and by Haas (1972). A fitted curve is consistent with all reversals (Fig. 6).

#### Modeled phase diagrams

For all reactions other than those mentioned previously,  $\Delta G_r$  and the location of the reactions in pressure-temperature space were calculated by addition and/or subtraction of the experimentally-determined values by the schemes noted in Table 6. Uncertainties were calculated by summing the squares of the uncertainties of the reactions added/subtracted and taking the square root. Figures 7, 8, 9, and 10 are four models of the  $\text{Al}_2\text{O}_3\text{-SiO}_2\text{-H}_2\text{O}$  system based upon distinct combinations of experimental results (as noted in Table 6). All metastable curves have been left off the plots, and in addition, some solid-solid reactions are metastable with excess water.

The uncertainty in the location of a reaction is primarily a function of the uncertainty in the experimental results for most of the reactions studied. However, for solid-solid reactions in which  $\Delta V_r$  and  $\Delta S_r$  are small, the approximation of thermal expansivities and compressibilities may have in-

troduced large errors. In particular, the reaction  $Py = 4Q + 2Di$  has been omitted from models 3 and 4 for this reason. Calculations show it to lie at 150–250°C and 10–14 kbars for both models and to have a steep positive slope. (See also Vernon, 1975, Fig. 4.5, p. 104; after Wall and Essene, 1972.)

The major difference between the four topologies is the location of an invariant point at which the kaolinite breakdown reactions and the  $Ka + Q = Py + V$  reaction intersect. In model 1, the point is at very high pressures and does not appear on the phase diagram. For models 2 and 3 it is at progressively lower pressures, and in model 4 it does not exist above 0°C. Day (1976) has proposed that the invariant point lies at approximately 325°C and 2 kbar. We have no way to select among the four models thermodynamically and turn to field evidence to give us further information.

*Field occurrences*

Zen (1961) has reported 2-, 3-, and 4-phase assemblages within the  $Al_2O_3$ - $SiO_2$ - $H_2O$  system from pyrophyllite deposits in North Carolina; there are many other reports of similar assemblages within the literature. Most such natural assemblages yield little defin-

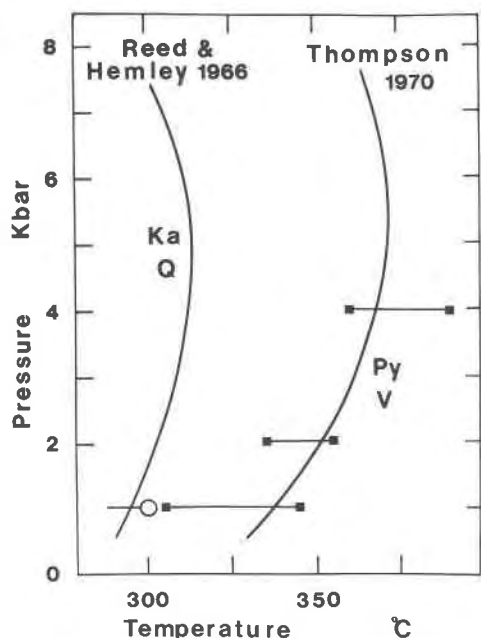


Fig. 4. The reaction  $Ka + 2Q = Py + V$ . The solid lines are consistent with available thermodynamic data. The point at 300°C represents the upper stability of kaolinite + quartz as determined by Reed and Hemley (1966).

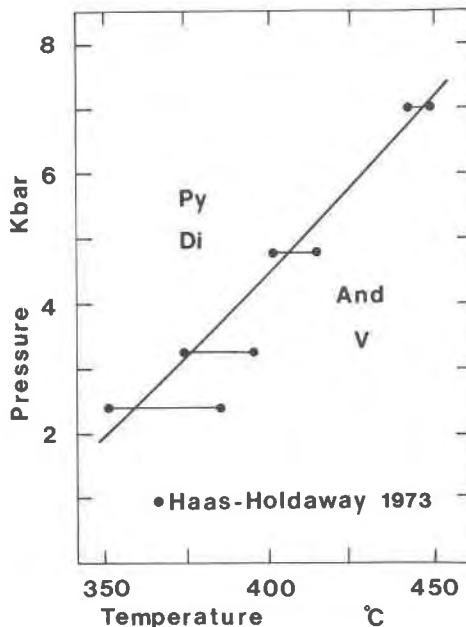


Fig. 5. The reaction  $Py + 6Di = 4And + 4V$ . The solid line is consistent with available thermodynamic data.

itive information, but several warrant special attention (Table 8).

In the presence of excess water, the stability of  $Al_2SiO_5$  is dependent upon reactions 7 and 8,  $Py + Di = Ky (And) + V$ . Although the exact locations of

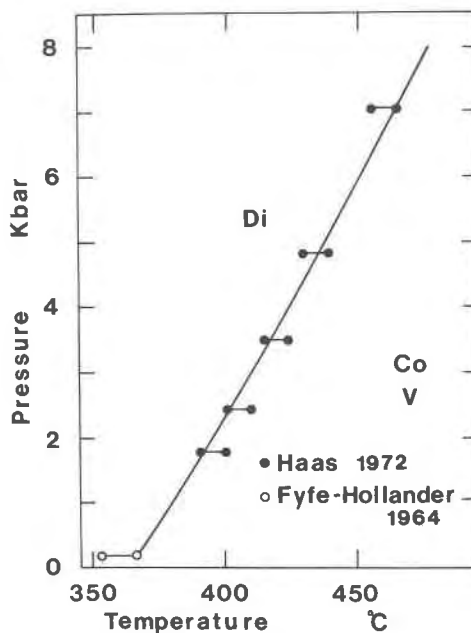


Fig. 6. The reaction  $2Di = Co + V$ . The solid line is consistent with thermodynamic data.



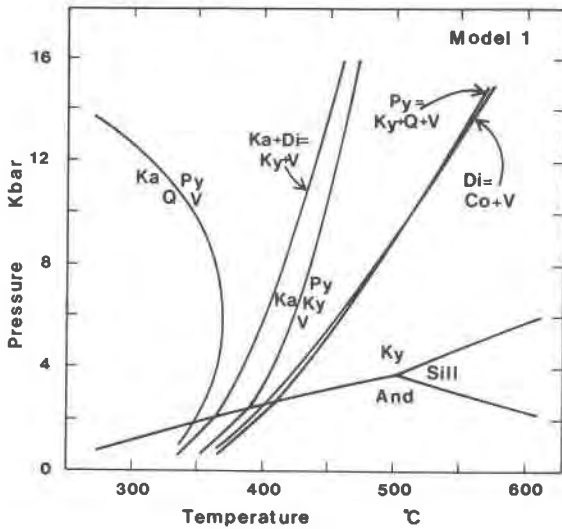


Fig. 7. The system  $\text{Al}_2\text{O}_3$ - $\text{SiO}_2$ - $\text{H}_2\text{O}$  based upon experimental results of Kerrick (1968) and Thompson (1970).

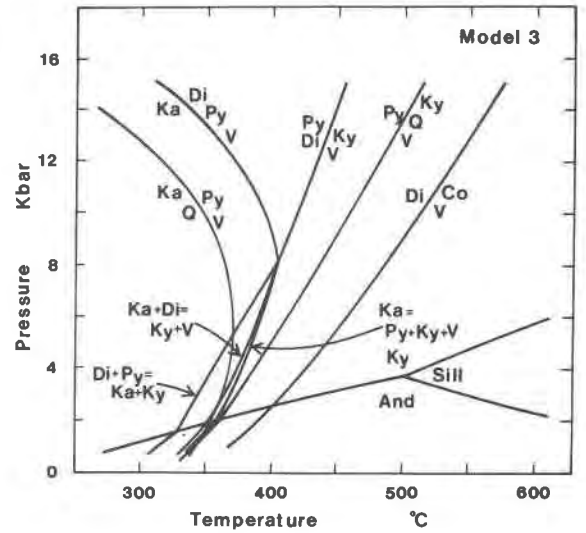


Fig. 9. The system  $\text{Al}_2\text{O}_3$ - $\text{SiO}_2$ - $\text{H}_2\text{O}$  based upon experimental results of Haas and Holdaway (1973) and Thompson (1970).

these reactions vary with fluid composition, models 1, 2, and 4 appear to be incompatible with  $\text{Ka} + \text{Q} + \text{Al}_2\text{SiO}_5$  assemblages (a, b, and e in Table 8). Model 3 will allow  $\text{Ka} + \text{Q} + \text{And}$  assemblages, and, if uncertainties in the locations of the reactions are considered,  $\text{Ka} + \text{Q} + \text{Ky}$  as well.

Assemblages f and i ( $\text{Py} + \text{Di} + \text{Ka}$  and  $\text{Py} + \text{Di}$ ) are limited by the reactions  $\text{Py} + \text{Di} = \text{Ky} + \text{V}$  and  $\text{Ka} = \text{Di} + \text{Py} + \text{V}$ . Neither assemblage is allowed by model 1; for models 2 and 3 minimum pressures of 10 and 8 kbar are indicated respectively, which are

far too high for the andalusite-bearing greenschist rocks that Zen studied, the  $\text{Py} + \text{Di} + \text{And}$  assemblage of Kerr (1932), and the pyrophyllite-diaspore rocks of Loughnan and Steggles (1976). Model 4, however, allows the assemblages to exist to low pressures. Similar observations were made by Day (1976).

As noted by Velde and Kornprobst (1969), by Wall and Essene (1972), and by Day (1976), the diaspore + quartz assemblage (h), of de Roever (1947), is stabilized by the reaction  $\text{Py} = \text{Di} + \text{Q}$ . As previously

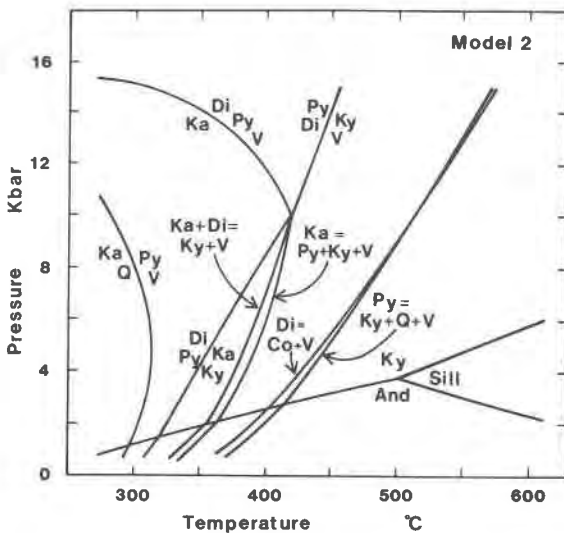


Fig. 8. The system  $\text{Al}_2\text{O}_3$ - $\text{SiO}_2$ - $\text{H}_2\text{O}$  based upon experimental results of Kerrick (1968) and Reed and Hemley (1966).

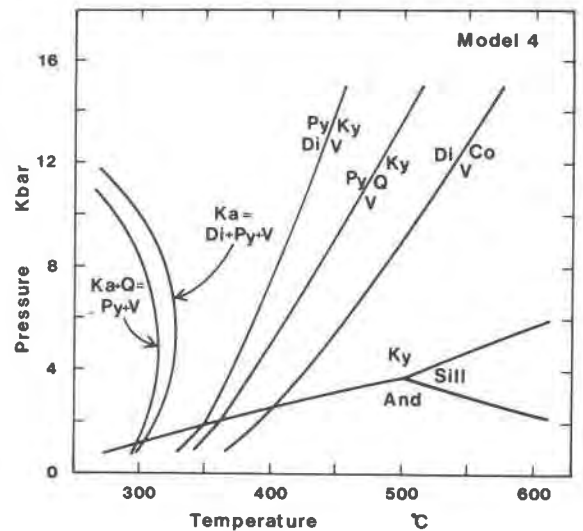


Fig. 10. The system  $\text{Al}_2\text{O}_3$ - $\text{SiO}_2$ - $\text{H}_2\text{O}$  based upon experimental results of Haas and Holdaway (1973) and Reed and Hemley (1966).

mentioned, errors in the estimation of the thermal expansivities and compressibilities of some of the phases may have introduced large errors in our calculations. Nonetheless, our calculated location for the reaction in models 3 and 4 (150–250°C and 10–14 kbar) is consistent with the jadeite–quartz assemblage, reported by de Roever to exist in rocks from his area. Reliable compressibility and expansivity values are necessary before this problem can be further clarified without accurate  $\Delta G_f$  data and/or direct experimental studies.

### Conclusion

Kerrick's (1968) experimental determination of the reaction  $\text{Py} = \text{And} + \text{Q} + \text{V}$  is the only common feature of models 1 and 2 that may account for their apparent nonvalidity. There is, however, no clear reason why Kerrick's results should be in error, and they are partially supported by Hemley's recent study. Nonetheless, the inconsistency of models 1 and 2 with common natural assemblages indicates that the models are in error.

Models 3 and 4 both have the same qualitative configuration as "semi-quantitative" model proposed by Day (1976). However, the lack of curvature in some of the reactions on his proposed phase diagram is inconsistent with current thermodynamic data and experimental studies; hence the specific locations of his reactions are questionable. The pressures required to stabilize diaspoire + pyrophyllite assemblages seem too high in model 3, although if one considers uncertainties in the locations of the univariant equilibria in that model, diaspoire + pyrophyllite assemblages could be stable at pressures of 4 kbar. Model 4 is unable to explain the rare andalusite + kaolinite + quartz assemblages, but kaolin could easily be introduced during alteration or retrogradation of an andalusite rock.

We conclude, therefore, that models 3 or 4 best approximate reality. These are consistent with known natural assemblages, current thermodynamic data and some of the experimental studies. This study, however, emphasizes the problems associated with modeling systems on thermodynamic data alone. Although our models are constrained to be consistent with experimental results as well as thermodynamic data, it is clear that they are still essentially qualitative. The problems stem from two sources: (1) contradictory experimental results, and (2) uncertainties associated with fitting curves to experimental data. Both of these problems can be resolved on the one

Table 8. Agreement between natural stable mineral assemblages in the  $\text{Al}_2\text{O}_3\text{-SiO}_2\text{-H}_2\text{O}$  system and predictions based on the four models of this paper

| Assemblage      | 1   | 2   | Model 3 | 4   | Source     |
|-----------------|-----|-----|---------|-----|------------|
| (a) Py-Ka-And-Q | no  | no  | yes     | no  | 1          |
| (b) Py-Ka-Ky-Q  | no  | no  | no      | no  | 1          |
| (c) Py-Ka-Q     | yes | yes | yes     | yes | 1, 2       |
| (d) And-Py-Q    | yes | yes | yes     | yes | 1          |
| (e) And-Ka-Q    | no  | no  | yes     | no  | 1          |
| (f) Py-Di-Ka    | no  | yes | yes     | yes | 1, 2       |
| (g) Py-Di-And   | no  | no  | no      | yes | 3          |
| (h) Di-Q        | no  | no  | yes     | yes | 4          |
| (i) Py-Di       | no  | yes | yes     | yes | 1, 2, 3, 5 |

- 1) Zen (1961)
- 2) Swindale and Hughes (1968)
- 3) Kerr (1932)
- 4) DeRoever (1947)
- 5) Kimizuka (1938)

hand by additional, accurate experiments, and on the other by a careful study of metamorphosed bauxite deposits, which evaluates equilibrium assemblages as well as the role of solid solutions and fluid compositions in a carefully calibrated pressure–temperature framework.

### Note added in proof

Chesworth (*Am. J. Sci.*, 278, 1018) has criticized Day's (1976) discussion of the stability of boehmite vs. that of diaspoire. Our results support Day's conclusion that "[diaspoire is the stable] aluminum hydrate species . . . at all geologically realizable conditions at which a hydrated phase is stable with respect to corundum and water."

### Acknowledgments

This research was supported in part by the Chemical Thermodynamics Program of the Chemistry Section of the National Science Foundation under contract GP-42525X to E. F. Westrum, Jr. We would like to thank Dr. R. A. Robie and Dr. B. S. Hemingway of the U. S. Geological Survey for allowing us to use their differential scanning calorimeter, and Albert Highe for assistance with the low-temperature heat-capacity measurements.

### References

- Brace, W. F., C. H. Scholz and P. N. Lamori (1969) Isothermal compressibilities of kyanite, andalusite and sillimanite from synthetic aggregates. *J. Geophys. Res.*, 74, 2089–2098.
- Burnham, C. W., J. R. Holloway and N. F. Davis (1969) Thermodynamic properties of water to 1,000°C and 10,000 bars. *Geol. Soc. Am. Spec. Pap.* 132.

- Clark, S. P., Jr. (1966) Handbook of physical constants. *Geol. Soc. Am. Mem.* 97.
- Day, H. W. (1975) The stability of gibbsite, boehmite, and diaspo-re (abstr.). *Geol. Soc. Am. Abstracts with Programs*, 7, 158.
- (1976) A working model of some equilibria in the system alumina-silica-water. *Am. J. Sci.*, 276, 1254-84.
- de Roever, W. P. (1947) Igneous metamorphic rocks in eastern central Celebes. In H. A. Brouwer, Ed., *Geological Explorations in the Island of Celebes*, p. 65-173. North Holland, Amsterdam.
- Ditmars, D. A. and T. B. Douglas (1971) Measurement of the relative enthalpy of pure  $\text{Al}_2\text{O}_3$  (NBS Heat capacity and enthalpy standard reference material No. 270) from 273 to 1173 K. *U. S. Natl. Bur. Stand. J. Res.*, 75A, 401-420.
- Ervin, G., Jr. and E. F. Osborn (1951) The system  $\text{Al}_2\text{O}_3\text{-H}_2\text{O}$ . *J. Geol.*, 59, 381-394.
- Fyfe, W. S. and M. A. Hollander (1964) Equilibrium dehydration of diaspo-re at low temperatures. *Am. J. Sci.*, 262, 709-712.
- Haas, H. (1972) Diaspo-re-corundum equilibria determined by epitaxis of diaspo-re on corundum. *Am. Mineral.*, 57, 1375-1385.
- and M. J. Holdaway (1973) Equilibria in the system  $\text{Al}_2\text{O}_3\text{-SiO}_2\text{-H}_2\text{O}$  involving the stability limits of pyrophyllite and thermodynamic data of pyrophyllite. *Am. J. Sci.*, 273, 449-461.
- Holdaway, M. J. (1971) The stability of andalusite and the aluminosilicate phase diagram. *Am. J. Sci.*, 271, 97-131.
- Kennedy, G. C. (1959) Phase relations in the system  $\text{Al}_2\text{O}_3\text{-H}_2\text{O}$  at high temperatures and pressures. *Am. J. Sci.*, 257, 563-573.
- Kerr, P. F. (1932) The occurrence of andalusite and related minerals at White Mountain, California. *Econ. Geol.*, 27, 614-643.
- Kerrick, D. M. (1968) Experiments on the upper stability limit of pyrophyllite at 1.8 kb and 3.9 kb pressure. *Am. J. Sci.*, 206, 204-214.
- Kimizuka, K. (1938) On the Reseki deposit (aggregation of pyrophyllite, kaolinite and diaspo-re) at Mituisi, Bizen Province, Japan. *Kyoto Imp. Univ., Coll. Sci. Mem., ser. B*, 14, 73-122.
- King, E. G., Barany, W. W. Weller and L. B. Pankratz (1967) Thermodynamic Properties of Forsterite and Serpentine. *U. S. Bur. Mines Rep. Inv.* 6962.
- Loughnan, F. C. and K. R. Steggle (1976) Cookeite and diaspo-re in the Back Creek pyrophyllite deposit near Pambula, N.S.W. *Mineral. Mag.*, 40, 765-772.
- Mukaiibo, T. A. and Y. Takahashi (1969) The heat capacity and heat of dehydration of the hydrated aluminas. *First Internatl. Conf. Calorim. Thermodyn., Warsaw*.
- Neuhaus, A. and H. Heide (1965) Hydrothermaluntersuchungen im System  $\text{Al}_2\text{O}_3\text{-H}_2\text{O(I)}$ : Zustandsgrenzen und Stabilitätsverhältnisse vom Böhmit, Diaspo-re, und Korund im Druckbereich > 50 bar. *Dtsch. Keram. Gesell. Ber.*, 42, 167-181.
- Reed, B. L. and J. J. Hemley (1966) Occurrence of pyrophyllite in the Kekiktuk conglomerate, Brooks Range, northeastern Alaska. *U. S. Geol. Surv. Prof. Pap.*, 550C, 162-166.
- Robie, R. A., P. M. Bethke and K. M. Beardsley (1967) Selected X-ray crystallographic data. *U. S. Geol. Surv. Bull.* 1248.
- and D. R. Waldbaum (1968) Thermodynamic properties of minerals and related substances at 298.15K and one atmosphere pressure and at higher temperatures. *U. S. Geol. Surv. Bull.* 1259.
- Rothbauer, V. R., F. Zigan, and H. O'Daniel (1967) Verfeinerung der Struktur des Bayerits,  $\text{Al(OH)}_3$ , Einschliesslich eines Vorschlags für die H-Positionen. *Z. Kristallogr.*, 125, 317-331.
- Rucklidge, J. C. and E. L. Gasparrini (1969) EMPADR VII, a Computer Program for Microprobe Data Reduction. Department of Geology, University of Toronto.
- Shomate, C. H. and O. A. Cook (1946) Low temperature heat capacities and high temperature heat contents of  $\text{Al}_2\text{O}_3 \cdot 3\text{H}_2\text{O}$  and  $\text{Al}_2\text{O}_3 \cdot \text{H}_2\text{O}$ . *J. Am. Chem. Soc.*, 68, 2140-2142.
- Stimson, H. E. (1961) Text revision of the international temperature scale of 1948. In C. M. Herzfeld, Ed., *Temperature Measurement and Control for Scientific Investigations*, Vol. 3, p. 547-579. Reinhold, New York.
- Swindale, L. D. and I. R. Hughes (1968) Hydrothermal association of pyrophyllite, kaolinite, diaspo-re, dickite and quartz in the Coromandel area. *New Zealand J. Geol. Geophys.*, 11, 1163-1183.
- Thompson, A. B. (1970) A note on the kaolinite-pyrophyllite equilibrium. *Am. J. Sci.*, 268, 454-458.
- Velde, B. and J. Kornprobst (1969) Stabilité des silicates d'alumine hydratés. *Contrib. Mineral. Petrol.*, 21, 63-74.
- Vernon, R. H. (1975) *Metamorphic Processes*. Wiley, New York.
- Wall, V. J. and E. J. Essene (1972) Subsolidus equilibria in  $\text{CaO-Al}_2\text{O}_3\text{-SiO}_2\text{-H}_2\text{O}$  (abstr.). *Geol. Soc. Am. Abstracts with Programs*, 4, 700.
- Westrum, E. F., Jr., G. T. Furukawa and J. T. McCullough (1968) Adiabatic low-temperature calorimetry. In J. T. McCullough and D. W. Scott, Eds., *Experimental Thermodynamics*, Vol. 1, p. 133-214. Butterworth, London.
- , E. J. Essene and D. Perkins, III (1979) Thermophysical properties of the garnet, grossularite,  $(\text{Ca}_3\text{Al}_2\text{Si}_3\text{O}_{12})$ . *J. Chem. Thermodyn.*, 11, 57-66.
- Zen, E-an (1961) Mineralogy and petrology of the system  $\text{Al}_2\text{O}_3\text{-SiO}_2\text{-H}_2\text{O}$  in some pyrophyllite deposits of North Carolina. *Am. Mineral.*, 46, 52-66.

Manuscript received, July 21, 1977;  
accepted for publication, May 17, 1978.